MAYO CLINIC

BRIEF REPORT

Remission of Disseminated Cancer After Systemic Oncolytic Virotherapy

Stephen J. Russell, MD, PhD; Mark J. Federspiel, PhD; Kah-Whye Peng, PhD; Caili Tong, MS; David Dingli, MD, PhD; William G. Morice, MD, PhD; Val Lowe, MD; Michael K. O'Connor, PhD; Robert A. Kyle, MD; Nelson Leung, MD; Francis K. Buadi, MD; S. Vincent Rajkumar, MD; Morie A. Gertz, MD; Martha Q. Lacy, MD; and Angela Dispenzieri, MD

Abstract

MV-NIS is an engineered measles virus that is selectively destructive to myeloma plasma cells and can be monitored by noninvasive radioiodine imaging of NIS gene expression. Two measles-seronegative patients with relapsing drug-refractory myeloma and multiple glucose-avid plasmacytomas were treated by intravenous infusion of 10^{11} $TCID_{50}$ (50% tissue culture infectious dose) infectious units of MV-NIS. Both patients responded to therapy with M protein reduction and resolution of bone marrow plasmacytosis. Further, one patient experienced durable complete remission at all disease sites. Tumor targeting was clearly documented by NIS-mediated radioiodine uptake in virus-infected plasmacytomas. Toxicities resolved within the first week after therapy. Oncolytic viruses offer a promising new modality for the targeted infection and destruction of disseminated cancer.

 ■ Mayo Clin Proc. 2014;■■(■):1-8

Oncolytic viruses (OVs) are promising experimental anticancer agents that, because of their complexity and diversity, can incorporate a variety of novel tumor-targeting and cell-killing mechanisms.[1] Oncolytic viruses have already shown clinical promise as immunotherapeutic agents, driving immune-mediated tumor destruction after intratumoral administration in patients with metastatic melanoma.[2,3] Also, there have been reports of localized tumors responding to an intravenously administered virus.[1] However, the "oncolytic paradigm," whereby a systemically administered OV targets a disseminated cancer and initiates a spreading infection that mediates the cancer's destruction, has not yet been clinically documented.[1]

Multiple myeloma (MM) is a malignancy of terminally differentiated plasma cells that diffusely infiltrate the bone marrow as well as form skeletal and/or soft tissue plasmacytomas (focal lesions). Multiple myeloma typically responds well to alkylator-, corticosteroid-, and immune-modulatory drugs and proteasome inhibitors but eventually becomes refractory to these treatments and is rarely cured.[4] New MM treatment modalities such as oncolytic virotherapy are therefore being actively explored.

MV-NIS is a recombinant oncolytic measles virus (MV) derived from an attenuated Edmonston lineage vaccine strain (MV-Edm) that was adapted to grow on human cancer (HeLa) cells, then engineered to express the human thyroidal sodium iodide symporter (NIS) so that its in vivo spread can be noninvasively monitored by radioiodine single-photon emission computed tomography (SPECT)—computed tomography (CT) imaging.[5] Measles is an enveloped lymphotropic paramyxovirus with a negative-sense RNA genome whose surface glycoproteins not only mediate the entry of the virus into susceptible target cells but also drive the fusion of infected cells with adjacent uninfected cells.[6] Unlike naturally occurring measles, MV-Edm, and hence MV-NIS, targets CD46 as a cell-entry and cell-fusion receptor.[5-7] CD46 is a ubiquitous complement regulatory protein that, fortuitously, is highly expressed on human myeloma cells, making them abnormally susceptible to MV-NIS infection, syncytium formation, and cell killing.[8]

The antimyeloma efficacy of systemic MV-NIS therapy was found to be dose dependent when the virus was administered intravenously in myeloma xenograft models.[7] Antitumor activity was lost in mice that were passively immunized with antimeasles antiserum.[9,10] MV-NIS

From the Department of Molecular Medicine (S.J.R., M.J.F., K.-W.P., C.T., D.D., A.D.), Division of Hematology (S.J.R., D.D., R.A.K., F.K.B., S.V.R., M.A.G., M.Q.L., A.D.), Department of Laboratory Medicine and Pathology (W.G.M., A.D.), Department of Radiology (V.L., M.K.O.), and Division of Nephrology and Hypertension (N.L.), Mayo Clinic, Rochester, MN.

toxicities were not encountered in preclinical dose-finding studies in CD46 transgenic mice and nonhuman primates, even at the maximum feasible intravenous dose.[7] A phase 1 clinical trial was therefore initiated to determine the maximum tolerated dose of intravenously administered MV-NIS in patients with advanced, refractory MM.[11] The trial, which is now almost completed and will be reported in detail elsewhere, has a standard cohorts-of-3 design with a first dose level of 10^6 $TCID_{50}$ (50% tissue culture infectious dose) of MV-NIS, increasing by 10-fold dose increments to a maximum feasible dose of 10^{11} $TCID_{50}$. Eligible patients had relapsing myeloma refractory to approved therapies.

In this current report, we provide preliminary data on 2 patients from the phase 1 trial. These patients were selected for immediate reporting because (1) they were the first 2 patients studied at the highest feasible dose level who were also seronegative for prior measles exposure and (2) they both had no response to multiple rounds of conventional therapy for MM and were therefore at risk for imminent death. Thus, these 2 patients provided a unique opportunity to determine the systemic adverse effects of oncolytic virotherapy in the absence of a preexisting antiviral immune response, as well as the resulting effect on tumor burden. Collectively, these patients provided heretofore unreported insights into the feasibility and risk-to-benefit profile of this novel approach to cancer therapy.

PATIENTS AND METHODS

Selected Study Patients

Patient 1. Patient 1 was a 49-year-old woman with heavily pretreated light chain MM who experienced relapse while receiving no therapy 9 months after her second autologous stem cell transplant (ASCT). Multiple myeloma had been diagnosed 9 years earlier and treated with thalidomide and dexamethasone followed by consolidative ASCT[12]; lenalidomide and dexamethasone[13]; cyclophosphamide, bortezomib, and dexamethasone[14]; and a second ASCT. Immediately before receiving MV-NIS, she had a rapidly enlarging firm, nontender 3-cm-diameter plasmacytoma emanating from the left frontal bone. The serum λ free light chain level had increased substantially from 2.5 to 8.0 mg/dL (to convert to mg/L, multiply by 10) since her previous clinic visit 2 months earlier. Positron emission tomography (PET)—CT revealed multifocal osseous progression of her MM when compared with the previous scan obtained immediately before her second ASCT, with enlargement of the glucose-avid lesion in the left frontal bone and new glucose-avid lesions in the left sternal manubrium, right frontal bone, medial right clavicle, and T11 vertebral body. Bone marrow biopsy, which had yielded completely negative results on day 100 following the ASCT, revealed 3% infiltration with λ light chain—restricted clonal plasma cells.

Patient 2. Patient 2 was a 65-year-old woman with relapsing IgA κ MM refractory to all approved antimyeloma drugs who experienced disease progression while receiving carfilzomib, pomalidomide, and dexamethasone therapy. Her MM had been diagnosed 7 years earlier and had been treated with local radiotherapy; high-dose dexamethasone; lenalidomide and dexamethasone; single-agent bortezomib; cyclophosphamide, bortezomib, and dexamethasone; ASCT; lenalidomide, bendamustine, and dexamethasone; bortezomib, cyclophosphamide, lenalidomide, and dexamethasone; carfilzomib plus dexamethasone; bortezomib, dexamethasone, thalidomide, cisplatin, doxorubicin, cyclophosphamide, and etoposide; and several experimental therapies. Before MV-NIS therapy, she had innumerable palpable (firm, nontender) soft tissue plasmacytomas, especially in the muscles of her lower extremities, ranging in diameter from 2 to 7 cm. Her hemoglobin level was 8.9 g/dL (to convert to g/L, multiply by 10), and her serum κ free light chain value had increased from 6.5 mg/dL to 31.1 mg/dL (to convert to mg/L, multiply by 10) over the previous month. PET-CT revealed numerous fluorodeoxyglucose (FDG)—avid nodules and mass lesions, most prominent below the level of the diaphragm and especially in the soft tissues of the legs. Several of these lesions had increased in size and FDG activity since the previous scan 6 weeks earlier. The largest lesion, located in the left hamstring musculature, measured 74 × 46 mm with a maximum standard uptake value of 8.0. Bone marrow biopsy revealed 1% infiltration with κ light chain—restricted clonal plasma cells.

Mayo Clin Proc. ■ XXX 2014;■■(■):1-8 ■ http://dx.doi.org/10.1016/j.mayocp.2014.04.003
www.mayoclinicproceedings.org

Virus Dose and Location of Infusion

In both patients, the virus, at a dose of 10^{11} $TCID_{50}$, was infused into a superficial arm vein in 100 mL of normal saline over 60 minutes.

Assessment of Response to Oncolytic Virotherapy

The following methods were used to assess the immediate and delayed effects of the virotherapy as well as its pharmacokinetic profile and its ability to target sites of tumor growth.

Measurement of Temperature, Heart Rate, and Blood Pressure. Measurement of physiologic variables during and immediately after virus infusion was performed with the patient in the sitting position. Heart rate was determined from the radial pulse, and blood pressure was determined from a mechanically cycled Philips IntelliVue MP50 sphygmomanometer. Sublingual temperature was measured using a Welch Allyn SureTemp Plus 690 Device.

Pharmacokinetic Studies. Blood samples for early pharmacokinetic studies were obtained at baseline, at 1, 30, 60, 120, and 240 minutes after completion of the MV-NIS infusion, and again on days 3, 8, 15, and 42. RNA was extracted and analyzed by quantitative reverse transcription—polymerase chain reaction to determine the number of circulating viral genomes (early time points) or *N* gene messenger RNA transcripts (later time points) in the blood at each time point.[7]

Antimeasles Antibody Titers. Neutralizing antimeasles antibody titers were determined using a standard plaque reduction neutralization assay in which serial dilutions of serum were mixed with 250 infectious units of an indicator virus (MV-GFP).[9]

SPECT-CT Imaging Studies. Radioiodine uptake was visualized on SPECT-CT obtained 6 hours after oral administration of 5 mCi of iodine 123. The scans were obtained at baseline and on days 8, 15, and 28 after virus administration using a Philips BrightView SPECT-CT scanner. To suppress thyroidal NIS expression, liothyronine sodium (25 μg, 3 times daily) was administered orally for 4 days before the first (baseline) scan and was continued until completion of the day 28 scan.

Eight-Color Plasma Cell Flow Cytometry. Mononuclear cells isolated from aspirated bone marrow by Ficoll gradient were stained with antibodies to CD38 (APC), CD138 (PerCP-Cy5.5), CD19 (PE-Cy7), and CD45 (APC-Cy7). They were then fixed-permeabilized and treated with RNAse, followed by staining with antibodies to κ (FITC) and λ (PE) immunoglobulin light chains and a 15-μM solution of 4′,6′-diamidino-2-phenylindole. A total of 500,000 events were collected on BD FACSCanto II instruments (BD Biosciences) and analyzed using BD FACSDiva software (BD Biosciences) for surface immunophenotype, cytoplasmic immunoglobulin light chain restriction, and DNA content and S phase through analysis of 4′,6′-diamidino-2-phenylindole staining.

RESULTS

Systemic Response to Virus Infusions

Patient 1. MV-NIS was infused into a superficial vein on the left forearm. The infusion time of 60 minutes included a brief interruption for severe headache that responded to diphenylhydramine and acetaminophen. Two hours later, the patient became febrile (temperature, 40.5°C), tachycardic (maximum heart rate, 175 beats/min), and hypotensive (minimum blood pressure, 73/33 mm Hg) with severe nausea and vomiting that responded to acetaminophen, meperidine, metoclopramide, lorazepam, and a cooling blanket. Fever recurred over the next few days, and a superficial venous thrombosis extending from the wrist to the upper humerus was detected. The thrombosis was managed conservatively and resolved over the ensuing weeks. At no time following administration of MV-NIS, nor for the preceding 9 months, did she receive corticosteroids or any drug with known antimyeloma activity.

Patient 2. MV-NIS was infused into a superficial forearm vein. Two hours after infusion, the patient became febrile (maximum temperature, 40.0°C), tachycardic (maximum heart rate, 119 beats/min), and hypotensive (minimum blood pressure, 85/44 mm Hg). The fever responded to acetaminophen. The hypotension was attributed to dehydration and was effectively treated

with intravenous hydration. Headache without neurologic deficit responded to intravenous morphine. Recurrences of fever during the first week after virus infusion resolved spontaneously within a few hours.

Antiviral Antibody Response

Neither of the patients had detectable neutralizing antimeasles antibodies before therapy, but both of them had high serum titers 6 weeks after virus administration (Table).

Effect on Tumor Burden

Response data are summarized in Figure 1. The level of the involved serum free light chain decreased considerably in both patients (Figure 1, A). In patient 1, the λ free light chain level declined rapidly into the reference range; it remained normal at 7 months after therapy but was minimally increased (2.9 mg/dL) 9 months posttherapy. In patient 2, the κ free light chain level decreased rapidly to 25% of its initial value, but this decline was not maintained at the 6-week time point. Bone marrow aspirates and biopsies were obtained 6 weeks after therapy and were compared with baseline samples (Figure 1, B). In both patients, the bone marrow plasmacytosis resolved completely, leaving no morphologic or immunophenotypic evidence of a plasma cell proliferative disorder in the posttherapy bone marrow samples. Thirty-six hours after MV-NIS infusion, patient 1 noted that the plasmacytoma on her left forehead had softened and started to shrink, and by 6 weeks, it was no longer palpable. Patient 2 also had the early impression that her plasmacytomas were shrinking, having become tender and painful 1 week after therapy, but by 6 weeks, there was no objective change in their size. Six weeks after therapy, FDG PET-CT scans were compared with baseline pretherapy scans (Figure 1, C). The scan in patient 1 showed substantial improvement in all 5 previously noted lesions. There was almost complete resolution of the FDG-avid soft tissue mass occupying the lytic lesion in the left frontal bone. Further, there was a considerable reduction of maximum standard uptake value in the lytic lesions in the right frontal bone, medial right clavicle, and sternum and resolution of the focus in vertebra T11. A repeated scan 6 months after therapy revealed minimal FDG uptake in the right frontal lesion and no discernible uptake in the remaining lesions. By 9 months after therapy, there was increasing FDG uptake in the right frontal lesion. Local radiotherapy was administered because the remainder of the skeletal lesions were FDG negative and on repeated bone marrow biopsy, results remained morphologically and immunophenotypically negative by flow cytometry. The 6-week posttherapy scan in patient 2 revealed increased size and FDG uptake in most of the soft tissue lesions, although a few lesions did have varying degrees of improvement, including resolution of a focus of uptake adjacent to the descending aorta and another in the lateral aspect of the right breast.

TABLE. Measles Genome Copy Numbers in Peripheral Blood After MV-NIS Infusion[a,b]

Variable	MV-N RNA copy number ($\times 10^3$/μg)	
	Patient 1	Patient 2
Time from infusion		
1 min	7650.0	317.0
30 min	890.0	401.0
60 min	2140.0	338.0
120 min	1270.0	307.0
240 min	638.0	173.0
Day 3	20.5	4.0
Day 8	5.2	17.9
Day 15	13.1	4.9
Day 42	4.9	0
3 mo	1.1	ND
5 mo	0	ND
PRN titer		
Pre-MV	<10.0	<10.0
Post-MV (day 42)	2560.0	320.0

[a]MV = measles virus; MV-N = measles virus *N* gene; ND = not done; PRN = plaque reduction neutralization.

[b]Antimeasles antibody titers were determined by PRN assay. The reciprocal of PRN titers is shown for before and after MV treatment.

SPECT-CT Imaging Studies to Monitor Virus Spread

MV-NIS–infected cells express the thyroidal sodium iodide symporter (NIS) and therefore concentrate radioactive iodide. Radioiodine SPECT-CT scans from patients 1 and 2 provided clear evidence of tumor-targeted MV-NIS infection (Figure 2). Radioiodine uptake in the left frontal plasmacytoma of patient 1 was increased above background on the day 8 scan and was further increased on the day 15 scan (Figure 2, A), indicating propagation of the MV-NIS infection. However, there was

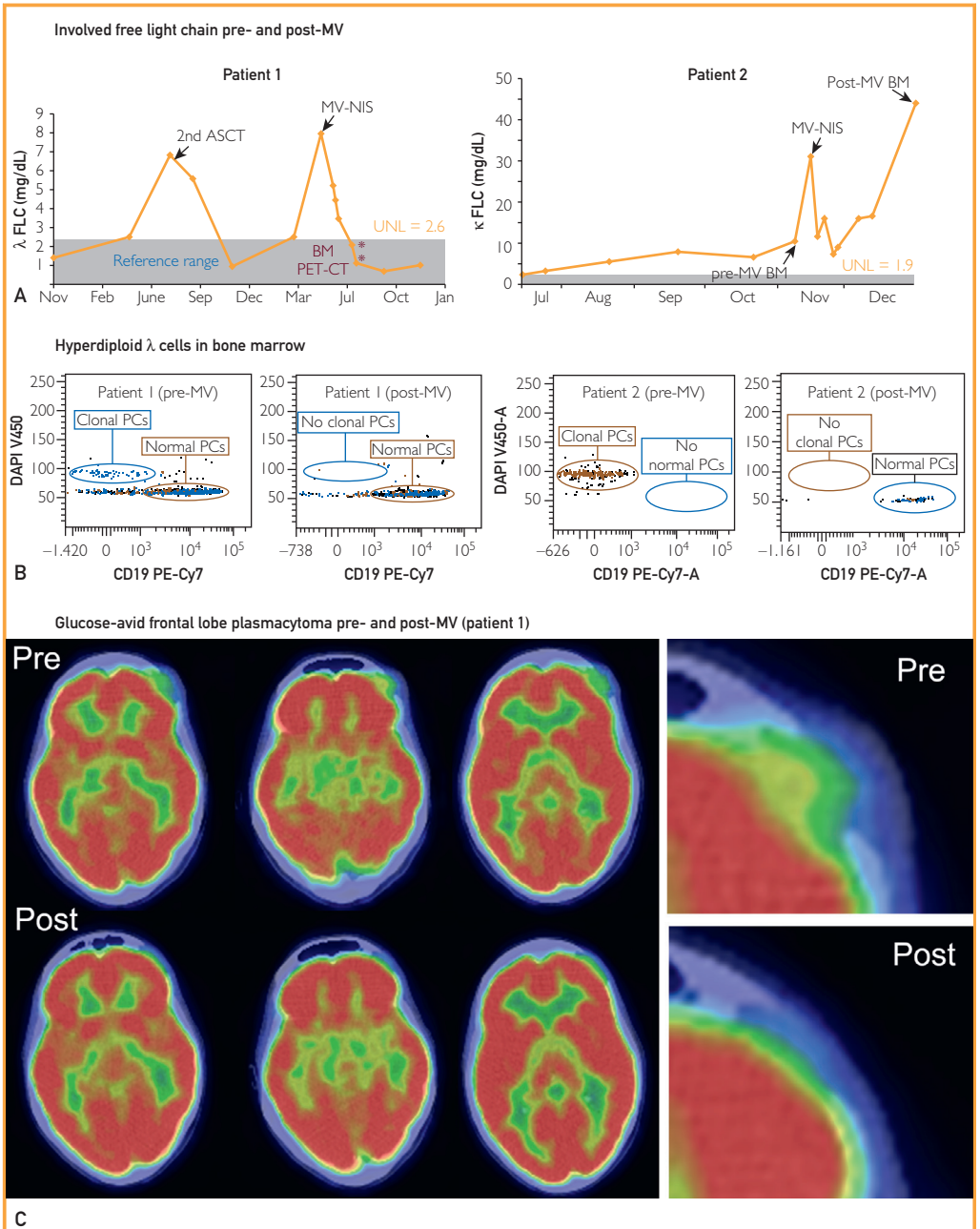

FIGURE 1. Clinical response to systemically administered MV-NIS. A, Serial free light chain (FLC) measurements in patients 1 and 2 as a surrogate of myeloma tumor burden, increasing at myeloma relapse and decreasing after successful therapy. Asterisks indicate the timing of relevant bone marrow (BM) and positron emission tomography–computed tomography (PET-CT) examinations. B, High-sensitivity 8-color plasma cell (PC) flow cytometry performed on pretherapy BM samples from both patients (left panels) shows CD38- and CD138-positive, CD19-negative monoclonal PCs (λ-restricted in patient 1, κ-restricted in patient 2) with hyperdiploid DNA content. In these same studies performed on BM samples obtained 6 weeks after therapy (right panels), the abnormal PCs are not present. C, Alternate coronal PET-CT sections at the level of the left frontal plasmacytoma in patient 1 before and 7 weeks after MV-NIS therapy. Far right panel shows higher magnification of the middle sections, focusing on the plasmacytoma. Note the pretherapy cerebral compression and altered skin contour that normalize after therapy. ASCT = autologous stem cell transplant; DAPI = 4′,6′-diamidino-2-phenylindole; MV = measles virus; UNL = upper normal limit.

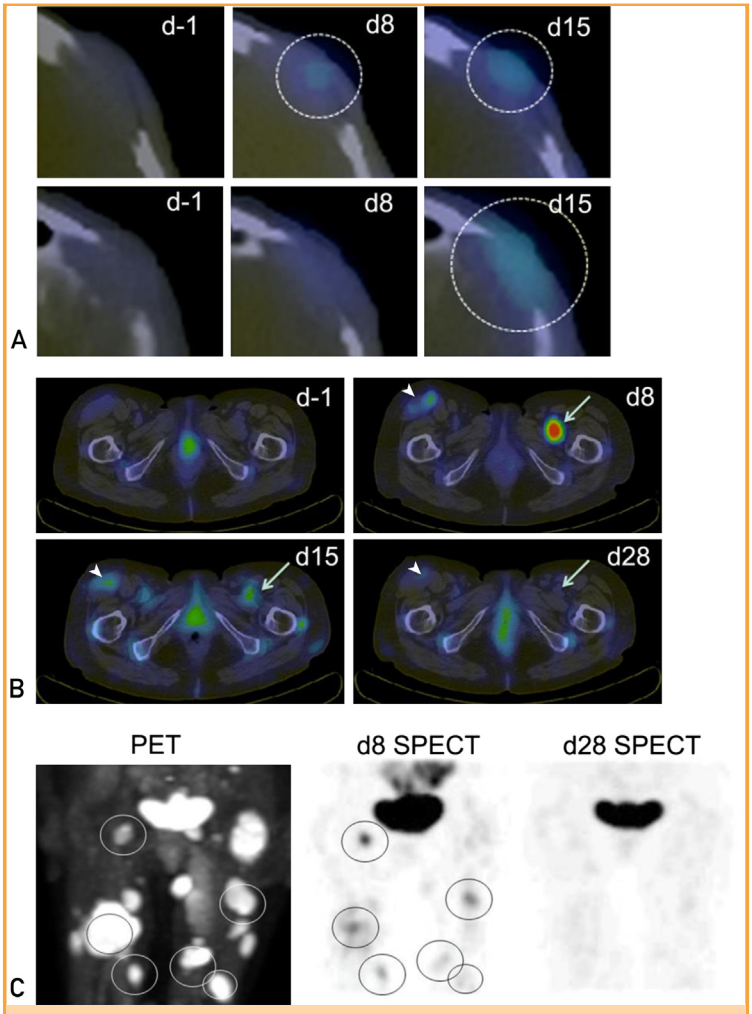

FIGURE 2. Intratumoral propagation of systemically administered MV-NIS. A, Serial single-photon emission computed tomography (SPECT)—computed tomography (CT) images from patient 1 at baseline (d-1) and on days 8 (d8) and 15 (d15) after MV-NIS infusion at the level of the left frontal plasmacytoma. Two adjacent transaxial slices from 6 hours after isotope administration are shown for each time point. There is a small area of increased uptake in the plasmacytoma visible in the lower slice on the day 8 scan (circle). This area of increased uptake is more extensive, and visible in both slices (circles), on the day 15 scan. B, Serial SPECT-CT images from patient 2 at baseline and on days 8, 15, and 28 (d28) after MV-NIS infusion at the level of the inguinal region. Compared with the baseline images, there is greatly increased radioiodine uptake in a deep-seated intramuscular plasmacytoma in the right hemipelvis on day 8 after MV-NIS administration, which is diminishing by day 15 and is back to baseline by day 28 (arrows). On the same transaxial slices, there is moderately increased radioiodine uptake in the large left inguinal lymph node on day 8, which again is diminishing by day 15 and back to baseline by day 28 (arrowheads). C, Anteroposterior fluorodeoxyglucose positron emission tomography (PET)—CT image obtained before MV-NIS administration and the corresponding iodine 123 SPECT-CT images obtained 8 days and 28 days after virus administration. All areas of intense radioiodine uptake (aside from the bladder) in the day 8 SPECT-CT scan are seen to correspond to glucose-avid plasmacytomas in the PET-CT image (circles).

no evidence for virus spread from plasmacytomas to adjacent normal tissues. In patient 2, the day 8 scan revealed striking radioiodine uptake in several plasmacytomas that was not present at baseline. Uptake diminished considerably by day 15 and was no longer detectable on day 28 posttherapy (Figure 2, B). Comparing day 8 radioiodine SPECT-CT and baseline FDG PET-CT scans, there was variable uptake of radioiodine by tumors of similar size (Figure 2, C), indicating heterogeneity of viral propagation in different plasmacytomas in the same patient.

DISCUSSION

We report the tumor-specific infection and clinical responses of the first 2 measles-seronegative patients with treatment-refractory myeloma to be treated intravenously with the oncolytic measles virus MV-NIS at the maximum feasible dose level. Targeted infection of virus-infected plasmacytomas was clearly documented (using SPECT-CT imaging in both patients) by the appearance and later disappearance of NIS-mediated radioiodine uptake signals that were absent at baseline. After virotherapy, NIS expression was heterogeneous among the plasmacytomas of patient 2. Resolution of bone marrow plasmacytosis and regression of identifiable plasmacytomas in patient 1 led to complete disease remission that lasted 9 months. This response occurred after only a single intravenous administration of the virus. Bone marrow plasmacytosis resolved in patient 2 and remained undetectable at 6 weeks after therapy, but her plasmacytomas were progressing by that time, and her free light chain level was increasing.

Despite the long history of the field of oncolytic virotherapy, complete remission of a disseminated malignancy mediated by a systemically administered virus has not previously been documented in a human subject, nor has the specific targeting of OV infection to sites of tumor growth. Although there have been many well-documented immune-mediated complete remissions (most frequently of metastatic MM) after intratumoral OV administration,[3] this has not been the case for intravenous virotherapy.[1] Another OV (vaccinia virus JX-594) was recently recovered from biopsied tumors following intravenous delivery in a phase 1 clinical trial,[15] but only one partial clinical response at a single tumor site was seen at the highest dose level

(approximately 10^9 $TCID_{50}$) in that study, and virus biodistribution was not evaluated because, unlike MV-NIS, the virus was not designed for noninvasive imaging. The current report is therefore the first to establish feasibility of the systemic oncolytic virotherapy paradigm.

In contrast to conventional drug therapies, OVs are designed to self-amplify at sites of tumor growth, which greatly complicates the study of their pharmacology. In the case of MV-NIS, this concern was addressed by engineering the virus to drive high-level NIS reporter gene expression in infected target cells such that its biodistribution and pharmacokinetics can be noninvasively monitored by radioiodine imaging.[5] Preclinical studies have also found that the antimyeloma potency of MV-NIS can be synergistically boosted by appropriately timed administration of iodine 131, which localizes to intratumoral sites of virus propagation depositing a tissue-destructive dose of beta radiation.[5] Based on the clinical outcome and imaging data, particularly from patient 2, there is now a strong rationale for combining MV-NIS with iodine 131 (radiovirotherapy) in a future clinical trial.

One key factor that may have contributed to the successful outcome in these 2 patients was their low pretreatment serum titers of antimeasles antibodies.[9,10,16-18] Another factor of probable relevance was the high dose of virus administered. Dose-response relationships for antitumor efficacy and virus delivery have been well documented in previous virotherapy studies,[7,15,19,20] and a dose-threshold effect can be mathematically predicted.[20] Also, measles virus transcripts were still detectable in the circulating cells of patient 1 at 6 weeks after virus infusion, by which time there had been a substantial boost to her antimeasles antibody titer, suggesting the possibility of continuing ongoing oncolytic activity even at that late time.

CONCLUSION

On the basis of this demonstration of tumor-selective MV-NIS replication and, in one case, durable tumor regression in heavily pretreated patients who have myeloma with bulky disease, OVs offer a promising new modality for the targeted infection and destruction of disseminated cancer. Additional MV-NIS is now being manufactured to support a planned phase 2 expansion of the clinical trial in measles-seronegative patients.

ACKNOWLEDGMENTS

We thank Kaaren K. Reichard, MD, for flow cytometric analysis of bone marrow.

Abbreviations and Acronyms: **ASCT** = autologous stem cell transplant; **Edm** = Edmonston; **FDG** = fluorodeoxyglucose; **GFP** = green fluorescent protein; **M-protein** = monoclonal protein; **MM** = multiple myeloma; **MV** = measles virus; **MV-NIS** = measles virus encoding human sodium iodide symporter; **NIS** = sodium iodide symporter; **OV** = oncolytic virus; **PET** = Positron emission tomography; **PRN** = plaque reduction neutralization; **SPECT** = single-photon emission computed tomography; **TCID50** = 50% tissue culture infectious dose

Grant Support: This work was supported by funds from the National Institutes of Health/National Cancer Institute (grants R01CA125614 and R01CA168719), Al and Mary Agnes McQuinn, the Harold W. Siebens Foundation, and the Richard M. Schulze Family Foundation. The National Cancer Institute RAID (Rapid Access to Intervention Development) Program supported MV-NIS manufacture and toxicology/pharmacology studies.

Potential Competing Interests: Drs Russell, Federspiel, and Peng and Mayo Clinic have a financial interest in the technology used in this research.

Correspondence: Address to Angela Dispenzieri, MD, Division of Hematology, Mayo Clinic, 200 First St SW, Rochester, MN 55905 (Dispenzieri.angela@mayo.edu).

REFERENCES

1. Russell SJ, Peng KW, Bell JC. Oncolytic virotherapy. *Nat Biotechnol*. 2012;30(7):658-670.
2. Vacchelli E, Eggermont A, Sautès-Fridman C, et al. Trial watch: oncolytic viruses for cancer therapy. *Oncoimmunology*. 2013;2(6):e24612.
3. Tong AW, Senzer N, Cerullo V, Templeton NS, Hemminki A, Nemunaitis J. Oncolytic viruses for induction of anti-tumor immunity. *Curr Pharm Biotechnol*. 2012;13(9):1750-1760.
4. Kyle RA, Rajkumar SV. An overview of the progress in the treatment of multiple myeloma. *Exp Rev Hematol*. 2014;7(1):5-7.
5. Dingli D, Peng KW, Harvey ME, et al. Image-guided radiovirotherapy for multiple myeloma using a recombinant measles virus expressing the thyroidal sodium iodide symporter. *Blood*. 2004;103(5):1641-1646.
6. Bellini WJ, Rota JS, Rota PA. Virology of measles virus. *J Infect Dis*. 1994;170(suppl 1):S15-S23.
7. Myers RM, Greiner SM, Harvey ME, et al. Preclinical pharmacology and toxicology of intravenous MV-NIS, an oncolytic measles virus administered with or without cyclophosphamide. *Clin Pharmacol Ther*. 2007;82(6):700-710.
8. Ong HT, Timm MM, Greipp PR, et al. Oncolytic measles virus targets high CD46 expression on multiple myeloma cells. *Exp Hematol*. 2006;34(6):713-720.
9. Ong HT, Hasegawa K, Dietz AB, Russell SJ, Peng KW. Evaluation of T cells as carriers for systemic measles virotherapy in the presence of antiviral antibodies. *Gene Ther*. 2007;14(4):324-333.
10. Liu C, Russell SJ, Peng KW. Systemic therapy of disseminated myeloma in passively immunized mice using measles virus-infected cell carriers. *Mol Ther*. 2010;18(6):1155-1164.
11. Vaccine Therapy With or Without Cyclophosphamide in Treating Patients With Recurrent or Refractory Multiple Myeloma.

ClinicalTrials.gov Identifier: NCT00450814. ClinicalTrials.gov website. http://clinicaltrials.gov/show/NCT00450814%20MC038C%20P30CA015083%20MC038C%2006-005263%20NCI-2009-01194%20NCT00450814. Updated March 20, 2014. Accessed April 14, 2014.

12. Mikhael JR, Dingli D, Roy V, et al. Management of newly diagnosed symptomatic multiple myeloma: updated Mayo Stratification of Myeloma and Risk-Adapted Therapy (mSMART) consensus guidelines 2013. *Mayo Clin Proc*. 2013;88(4):360-376.
13. Rajkumar SV, Jacobus S, Callander NS, et al; Eastern Cooperative Oncology Group. Lenalidomide plus high-dose dexamethasone versus lenalidomide plus low-dose dexamethasone as initial therapy for newly diagnosed multiple myeloma: an open-label randomised controlled trial [published correction appears in *Lancet Oncol*. 2010;11(1):14]. *Lancet Oncol*. 2010;11(1):29-37.
14. Reeder CB, Reece DE, Kukreti V, et al. Cyclophosphamide, bortezomib and dexamethasone induction for newly diagnosed multiple myeloma: high response rates in a phase II clinical trial. *Leukemia*. 2009;23(7):1337-1341.
15. Breitbach CJ, Burke J, Jonker D, et al. Intravenous delivery of a multi-mechanistic cancer-targeted oncolytic poxvirus in humans. *Nature*. 2011;477(7362):99-102.
16. Power AT, Wang J, Falls TJ, et al. Carrier cell-based delivery of an oncolytic virus circumvents antiviral immunity. *Mol Ther*. 2007;15(1):123-130.
17. Alcayaga-Miranda F, Cascallo M, Rojas JJ, Pastor J, Alemany R. Osteosarcoma cells as carriers to allow antitumor activity of canine oncolytic adenovirus in the presence of neutralizing antibodies. *Cancer Gene Ther*. 2010;17(11):792-802.
18. Guo ZS, Parimi V, O'Malley ME, et al. The combination of immunosuppression and carrier cells significantly enhances the efficacy of oncolytic poxvirus in the pre-immunized host. *Gene Ther*. 2010;17(12):1465-1475.
19. Berry LJ, Au GG, Barry RD, Shafren DR. Potent oncolytic activity of human enteroviruses against human prostate cancer. *Prostate*. 2008;68(6):577-587.
20. Bailey K, Kirk A, Naik S, et al. Mathematical model for radial expansion and conflation of intratumoral infectious centers predicts curative oncolytic virotherapy parameters. *Plos One*. 2013;8(9):e73759.